Supersonic Jet Studies on the Photophysics of Substituted Benzenes and Naphthalenes

Shuo Jiang and Donald H. Levy*

The James Franck Institute and The Department of Chemistry, University of Chicago, Chicago, Illinois 60637

Received: March 14, 2002; In Final Form: July 5, 2002

Laser-induced fluorescence (LIF) studies of seven substituted benzene and naphthalene derivatives seeded in a supersonic jet are reported. Dual fluorescence has been observed in aniline, 4-aminobenzonitrile, 1-aminonaphthalene, and 1-cyano-4-aminonaphthalene. The dual fluorescence is comprised of sharp features from a locally excited state and an unstructured, red-shifted background from a state that may be a mixed L_a/CT state. In aniline and 4-aminobenzonitrile the unstructured background is absent when low vibronic levels are excited but appears when higher levels are excited. In 1-aminonaphthalene and 1-cyano-4-aminonaphthalene, the background is observable upon excitation of all vibronic levels including the zero-point level. In all of the molecules, the intensity of the background increases with respect to that of the sharp component as the excitation energy is increased. The background becomes the only observable feature in the spectra at high excess energy. The broadening and red shift of the band center is difficult to explain solely by internal vibrational relaxation (IVR). It is attributed in part to emission from another electronic excited state with perhaps some charge-transfer character.

1. Introduction

The electronic structure of substituted benzenes and naphthalenes has been a subject of interest for almost a century and provides a test for molecular orbital theory.[1] If the substituents have electron-donating (such as $-NH_2$, $-OH$ groups) or electron-withdrawing properties (such as $-CN$, $-NO_2$ groups), the excited electronic states of substituted aromatic molecules may have charge-transfer character and large dipole moment. Molecules in this strongly polar state are highly reactive and play an important role in many mechanisms in photochemistry and photobiology. For example, in the bichromophoric systems used to study electronic energy transfer (EET) and photoinduced electron transfer (PET), substituted aromatic molecules such as electron donating aniline and electron withdrawing aminobenzonitrile act as a donor or acceptor.[2,3] A better understanding of the electronic structures of such substituted molecules may improve our understanding of the mechanisms in EET and PET.

The excited electronic state in such substituted molecules may have contributions from several electronic configurations. The important ones in the language of molecular orbital theory are the following: $\pi_{ring} \rightarrow \pi_{ring}^*$, $\pi_{ring} \rightarrow A^*$, and $D \rightarrow \pi_{ring}^*$, where π_{ring} and π_{ring}^* are bonding and antibonding orbitals of the aromatic ring, A^* is the antibonding orbital of the electron withdrawing group (such as the antibonding π orbital in $-CN$), and D is the bonding or nonbonding orbital of the donor (such as the lone pair electrons in $-NH_2$). The interactions among these configurations largely depend on their energy and symmetry.

In most cases the lowest excited electronic state in these substituted benzenes and naphthalenes is the $\pi_{ring} \rightarrow \pi_{ring}^*$ state, ^1L_b. Molecules in this state have a geometry similar to that of the ground state, and such an excited electronic state is designated the locally excited (LE) state in the literature. The higher excited electronic states may have contributions from all $\pi_{ring} \rightarrow \pi_{ring}^*$, $\pi_{ring} \rightarrow A^*$, and $D \rightarrow \pi_{ring}^*$ type configurations. The state consisting mainly of $\pi_{ring} \rightarrow \pi_{ring}^*$ type is ^1L_a (the second $\pi_{ring} \rightarrow \pi_{ring}^*$ excited state in Platt's nomenclature), and the ones consisting mainly of $\pi_{ring} \rightarrow A^*$ and $D \rightarrow \pi_{ring}^*$ type are charge-transfer (CT) states. The geometry of molecules in a CT state usually differs from that of the ground state because of its different electron distribution. Because of the change of geometry, optical excitation of a CT state is to highly excited vibrational levels and therefore occurs at significantly higher energy than excitation of an LE state. However, the CT state may be prepared through internal conversion from vibronic levels of the LE state. (A few examples of direct excitation to a charge-transfer state exist in cases where the state becomes the lowest excited state in some molecular systems.[4,5])

One of the early systematic studies of the charge-transfer character in electronic states in substituted aromatic molecules was conducted by McGlyn et al.,[6] in which a series of benzene derivatives in various solvents were studied through UV−Vis spectroscopy. The authors found that the ^1L_a state had large charge-transfer character. Its energy was sensitive to substitution and decreased as the polarity of the molecule increased. Thus, E (^1L_b) was less than E (^1L_a) in weakly polar molecules but E (^1L_b) was greater than E (^1L_a) in highly polar molecules. A great deal of research has also been performed on substituted molecules in the gas phase, especially in supersonic jet expansions. The cold isolated molecules prepared in a supersonic expansion provide an ideal system for the study of molecular electronic structure and intramolecular dynamics, notably radiationless transitions and intramolecular vibrational relaxation (IVR). In addition, the ability to prepare the molecules in a single vibronic level in the excited-state allows the investigation of state selectivity in such dynamics.

One substituted benzene, dimethylaminobenzonitrile (DMABN), has been subjected to extensive studies in both condensed and gas phase because of the possible low-lying CT state in this molecule.[7] DMABN exhibits dual fluorescence in polar solvents. It consists of a normal fluorescence that is almost the mirror image of the absorption spectrum and a red-shifted component.[8] The normal fluorescence is attributed to emission from a locally excited state, and the red-shifted fluorescence is

10.1021/jp025764a CCC: $22.00
Published on Web 08/13/2002

from a charge-transfer state.[9] Subsequent supersonic jet studies on DMABN and related derivatives, such as aminobenzonitrile (ABN),[10−13] showed no red-shifted emission from excited vibronic levels. It was concluded that the CT state in DMABN is high above the S_1 state in an isolated molecule, but it is stabilized by polar solvents in solution. The geometry of DMABN in the CT state has been the focus of extensive studies. The most popular one is the TICT model proposed by Grabowski.[9] It is challenged recently by the PICT model proposed by Zachariasse et al.[14]

Mordzinski et al.[15] of this lab studied 4-tolunitrile and benzonitrile in a supersonic jet. The fluorescence emission from the excited vibronic states has two components. At low excitation energies, the emission is comprised of sharp resonance features that resemble 0−0 emission. This was assigned to emission from a locally excited state. The other emission is broad, red-shifted, and unstructured. At low excitation energies, it appears only as a background but increases in intensity at high excitation energies. Eventually the broad unstructured band dominates the spectrum. Mordzinski et al. attributed the broad band to emission from a charge-transfer state lying close in energy to the locally excited state. Similar fluorescence behavior was observed in aminobenzonitrile by Yu et al.[11d] However, the authors argued that the decrease of sharp resonant features and increase of the broad background with increasing excitation energy was due to IVR. Sakota et al. attributed the red-shifted emission to spectral congestion.[16] They observed bands up to vibronic excitation energies of 942 cm^{-1} in benzonitrile and 763 cm^{-1} in tolunitrile, but did not examine emission from the more highly excited vibronic levels reported in ref 15.

The argument of Morzinski et al. was supported at that time by the ab initio calculations of Sobolewski et al.[17] They showed that a CT state was stabilized along the cyano group in-plane bending coordinate and its minimum is only 0.2 eV above the $S_1(\pi \rightarrow \pi^*)$. However, their later calculations with a large basis set and a more accurate method did not confirm this.[18] The origin of the broad, red-shifted emission observed in benzonitrile, tolunitrile, and aminobenzonitrile is still an open question. Is it emission from another excited electronic state that is populated through internal conversion from high-energy vibronic states in a locally excited state? Is it due to IVR within a locally excited state? And if it is from another electronic state, then what is nature of this state? Does it have large charge-transfer character? Why does it lie close in energy with the locally excited state?

To answer the above questions, a series of substituted benzenes and naphthalenes were studied in a supersonic jet by laser-induced fluorescence (LIF). The molecules chosen were 4-fluorobenzonitrile (4-FBN), *p*-dicyanobenzene (*p*-DCB), aniline, and 4-aminobenzonitrile (4-ABN) for the benzene system, and 1-cyanonaphthalene (1-CNN), 1-aminonaphthalene (1-AMN),- and 1-amino-4-cyanonaphthalene (*p*-AMCNN) for the naphthalene system (Figure 1). Though some of these molecules were previously studied in a supersonic jet by other research groups, in this study we observed new phenomena and drew new conclusions.

2. Experimental Section

LIF in a supersonic jet is a well-established field; the principle and the experimental setup have been described in detail elsewhere,[19] and only a brief description is given here. The molecules were purchased from Aldrich and used without further purification. Samples were heated in a cylinder under high-pressure helium. The temperature of the solid sample was typically set at its melting point or 20−30° above it to attain significant vapor pressure. For a sample that is liquid at room temperature, such as aniline, no heating was required. Helium that passed through the sample cylinder and mixed with its vapor was expanded into vacuum through a pinhole. For a 50-μm pinhole, 200 psi of helium was applied to achieve sufficient cooling.

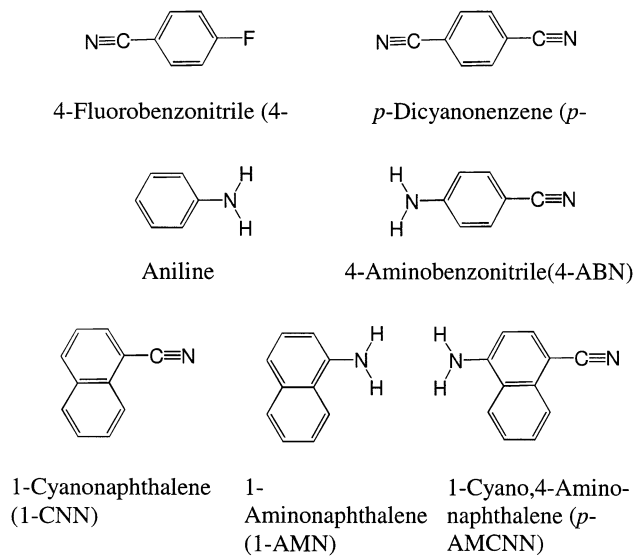

Figure 1. Formulas of substituted benzenes and naphthalenes.

The excitation laser was a Nd:YAG pumped dye laser, with a typical spectral resolution of 0.1 cm^{-1}. The laser beam crossed the supersonic jet about 1 cm downstream from the nozzle. The total fluorescence and dispersed fluorescence were collected perpendicular to the laser-jet plane by an *f*/1 lens system. Dispersed fluorescence spectra were recorded by passing the fluorescence through a 1 m monochromator with 4 Å/mm reciprocal dispersion. A photoelectron multiplier tube (EMI 9558QB) was used to detect the fluorescence. The signal from the photomultiplier was fed to an analogue to digital converter and was stored in a computer.

3. Results

3.1. Substituted Benzenes. The fluorescence excitation spectra of 4-fluorobenzonitrile (4-FBN), *p*-dicyanobenzene (*p*-DCB), aniline, and 4-aminobenzonitrile (4-ABN) are presented in Figure 2. The spectra agree well with what was reported in the literature for *p*-DCB,[20] aniline,[21,22] and 4-ABN.[11b,d] All four molecules show an intense 0−0 origin transition with well-resolved vibronic structure. The origin transitions for 4-FBN, *p*-DCB, aniline, and 4-ABN occur at 36619, 35113, 34029, and 33481 cm^{-1}, respectively. Some intense vibronic features are assigned on the basis of the previous studies of these molecules.[23] All the resolvable features were excited and dispersed fluorescence spectra were recorded. The representative ones marked with arrows in Figure 2 will be presented in the following section. The fact that all four molecules have intense origin transitions and lack long vibrational progressions indicates that the potential energy surface of the first excited electronic state is similar to that of the ground state.

3.1.1. 4-FBN. The dispersed fluorescence spectra obtained upon excitation of the vibrational peaks indicated by arrows in Figure 2a are displayed in Figure 3. The emission from these levels is "normal", in that it consists of sharp resonant features corresponding to transitions from localized vibronic levels of

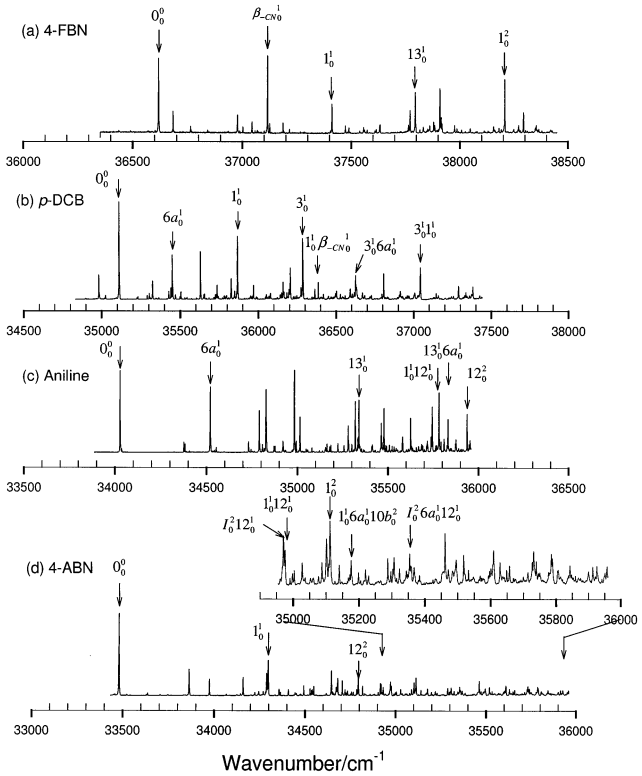

Figure 2. Fluorescence excitation spectra of substituted benzenes. (a) 4-fluorobenzonitrile; (b) *p*-dicyanobenzene; (c) aniline; (d) 4-aminobenzonitrile. The arrows mark the vibronic transition whose single vibronic level fluorescence spectra are presented in this paper. The assignment of the vibronic transitions is based on ref 22.

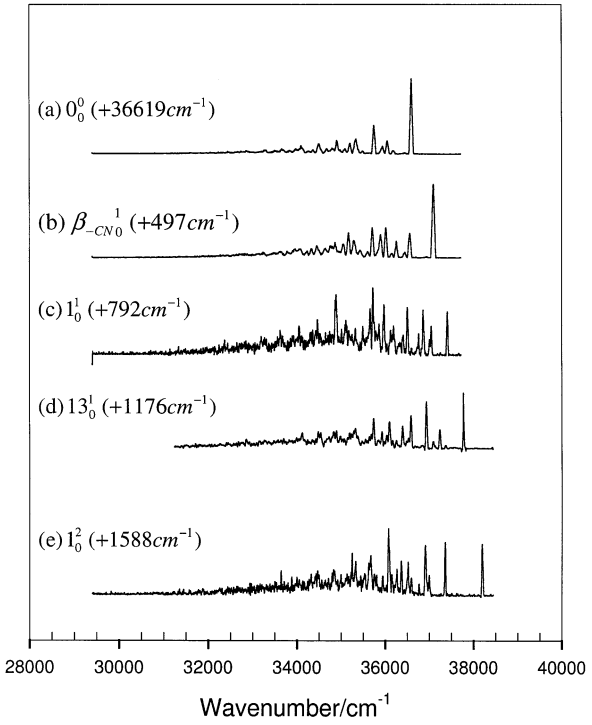

Figure 3. Dispersed fluorescence spectra of vibronic levels in 4-fluorobenzonitrile. The scattered light levels at the excitation wavenumbers are: (a) ∼2%; (b) ∼2%; (c) ∼15%; (d) ∼20%; (e) ∼10%.

the excited state to various levels of the ground state. No broad unstructured band was observed at excitation energies up to +1600 cm^{-1} above the origin. The small broad background in Figure 3c,e is probably due to IVR and spectral congestion.

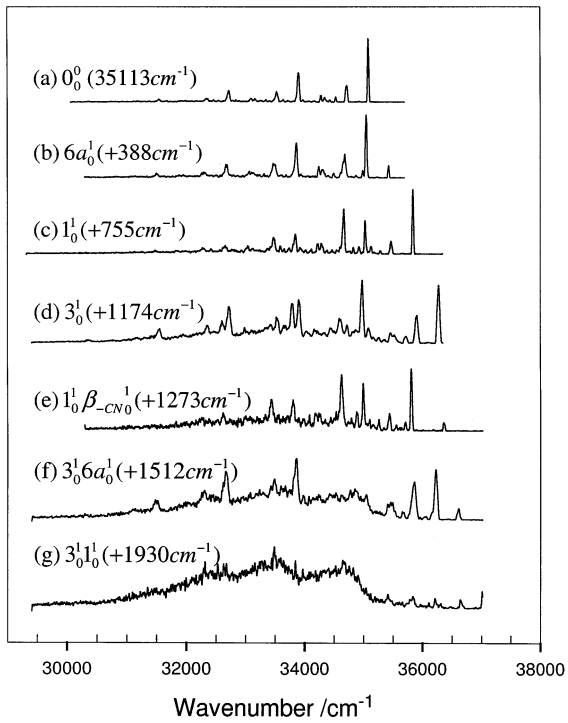

Figure 4. Dispersed fluorescence spectra of vibronic levels in *p*-dicyanobenzene. The scattered light levels at the excitation wavenumbers are: (a)−(e) ∼10%; (f and g) >50%.

The weakness of this background indicates that IVR and spectral congestion are minimal for 4-FBN.

3.1.2. p-DCB. The dispersed fluorescence spectra of *p*-DCB are displayed in Figure 4. Spectra 4a−c need little explanation. They illustrate emission from a localized vibronic level in S_1 to the ground state, dominated by $\Delta\nu = 0$ selection rules because of the similarity between ground and excited electronic states. The dispersed spectrum 4d obtained by exciting mode 3 shows considerable background relative to spectrum 4e. This is possibly due to vibronic coupling to a higher excited state. Mode 3 belongs to b_{3g} in a D_{2h} point group. It may gain transition probability via vibronic coupling to S_2 (L_a) which belongs to B_{1u}. The broad background increases by exciting higher energy combination bands involving mode 3 as shown in Figure 4f,g. The spectra here are largely broadened versions of the 0_0^0 emission, with resolvable but broadened vibronic features and a congested background. This is a signature of the onset of the IVR process.[24,25] So in *p*-DCB, the congested background is likely due to a combination of vibronic coupling to L_a and extensive IVR at high excess energies.

3.1.3. Aniline. There is a rich literature on studies of aniline, the most relevant to this work being the studies by Rice et al.,[22] Powers et al.,[21a] and Mikami et al.[21b] The fluorescence excitation in Figure 2c and dispersed fluorescence spectra in Figure 5a−c agree well with their studies. To the authors' knowledge, the dispersed fluorescence spectra 5d−f have not previously been reported. Though the $-NH_2$ group has an angle of 37° with the benzene ring in ground-state aniline,[22] the molecule is treated as belonging to a C_{2v} point group and as a result, the lowest excited state (^1L_b) belongs to $^1B_2$.

An interesting phenomenon was observed in the dispersed fluorescence spectra of aniline. The emission resulting from exciting vibrational features up to +1700 cm^{-1} in excitation energy all show primarily sharp resonant transitions between a localized vibronic level in ^1L_b to the ground state, with progressions in ring mode 6a and amino group inversion mode

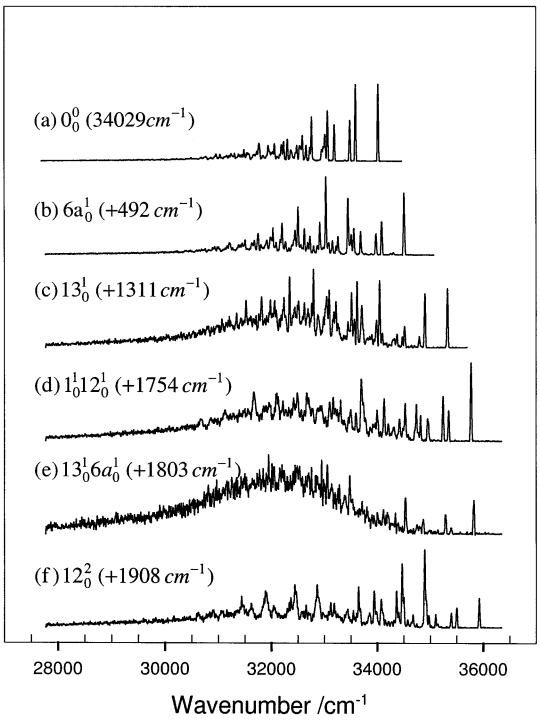

Figure 5. Dispersed fluorescence spectra of vibronic levels in aniline. The scattered light levels at the excitation wavenumbers are: (a and b) negligible; (c) ~10%; (d) ~10%; (e) ~100%; (f) ~30%.

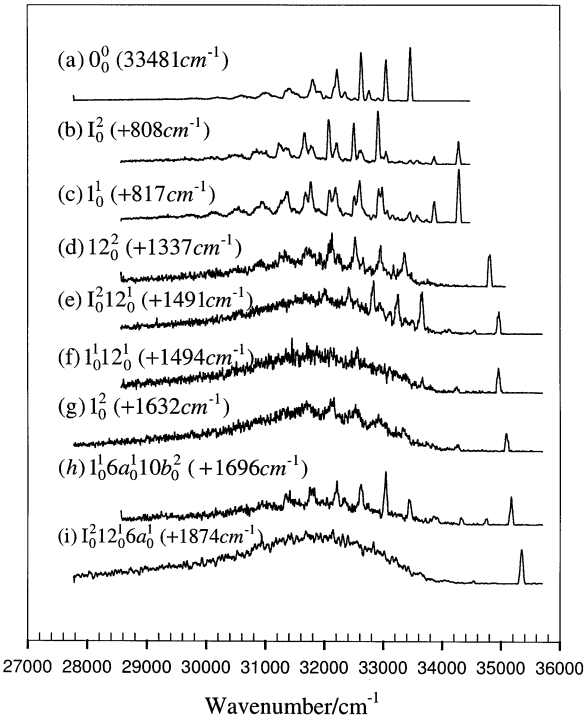

Figure 6. Dispersed fluorescence spectra of vibronic levels in 4-aminobenzonitrile. The scattered light levels at the excitation wavenumbers are: (a) negligible; (b) ~10%; (c) ~50%; (d) >50%; (e−i) ~100%.

I. The slight congested background in these spectra indicates that IVR and spectral congestion are not serious. The emission that results from exciting the $13^1 6a^1$ combination band which has only 50 cm^{-1} more excess energy is strikingly different from the others. A broad background centered about 2000 cm^{-1} to the red of the 0−0 transition is the most prominent feature, along with small amount of sharp resonant features from the localized level (Figure 5e). The dispersed spectrum resulting from exciting the next higher vibronic level in energy (12^2 in Figure 5f) becomes normal again, containing mostly sharp features. Exciting other higher vibronic levels all results in emission like that from $13^1 6a^1$ and those reported by Mordzinski et al.[15] in the benzonitrile study; the broad, red-shifted band is the dominant feature.

3.1.4. 4-ABN. As discussed in the Introduction, this molecule has been extensively studied both in solution and in the gas phase. Yu et al. examined dispersed fluorescence spectra upon exciting various vibronic levels of 4-ABN in a supersonic jet.[11d] The dispersed fluorescence spectra shown in Figure 6a−c were reported in Yu's study. Both Figures 6a and 6b agree with their results, but Figure 6c shown here has better resolution and signal-to-noise ratio. To the best of our knowledge, the rest of the spectra in Figure 6 were not previously reported.

The fluorescence excitation spectrum of 4-ABN is similar to that of aniline, except that it appears more congested in the high excess energy region, indicating vibronic coupling. The emission spectra display a similar pattern as those of aniline and benzonitrile. For excitation energy up to 1300 cm^{-1}, the spectra all look similar to the 0−0 emission with progressions in mode 6a and I and $\Delta\nu = 0$ for other modes, another indication that the two potential energy surfaces are similar. The doublet features in emission from 1^1 are a result of Fermi resonance between close lying 1^1 and I^2 vibronic levels (Figure 6b).

With increasing excitation energy, a broad background, red-shifted relative to origin, gains intensity. Spectra 6c−g can be best described as a superposition of resolved resonant features, similar to emission from lower vibronic levels, with a broad unstructured background. The ratio between the background and the resolved resonant features increases with excitation energy, but not monotonically at the beginning. This nonmonotonic behavior is similar to that observed with aniline. Besides the growing background, the individual resolved features are also more broadened with increasing excitation energy [compare those in Figure 6a,c,g). This trend is not monotonic either (compare those in Figure 6g,h). Exciting levels with >1800 cm^{-1} excess energy always results in spectra like 6g, with only a broad red-shifted band.

3.2. Substituted Naphthalenes. Figure 7 shows the fluorescence excitation spectra of 1-cyanonaphthalene (1-CNN), 1-aminonaphthalene (1-AMN), and 1-amino-4-cyanonaphthalene (*p*-AMCNN) up to 2000 cm^{-1} above the 0−0 transition. The strong transitions at 31415, 30045, and 29319 cm^{-1} are assigned to 0−0 transitions for 1-CNN, 1-AMN, and *p*-AMCNN, respectively. The fluorescence excitation spectrum of 1-CNN is similar to that reported by Saigusa et al.[26] and Lahmani et al.[27] Those of 1-AMN and *p*-AMCNN in a jet have not been reported before. Since the vibronic structure of substituted naphthalenes is not as well studied as that of the substituted benzenes, no attempt was made to fully assign the vibronic transitions in the excitation spectra. The vibronic assignment of 1-CNN in Figure 7a has been determined in previous studies.[27−29]

3.2.1. 1-CNN. The congested vibronic structure starting at about 1400 cm^{-1} above the origin (Figure 7a) is most likely due to vibronic mode mixing as a result of Fermi resonance and Duschinski effect.[29] The possible internal conversion between the S_1 (^1L_b) and S_2 (^1L_a) may also contribute to the congestion, since the S_1 (^1L_b) and S_2 (^1L_a) are separated by only about 2400 cm^{-1}.[30]

The dispersed fluorescence spectra of 1-CNN are shown in Figure 8. Figures 8a−c agree well with those previously reported.[27] The strongest bands in all these spectra are $\Delta\nu = 0$

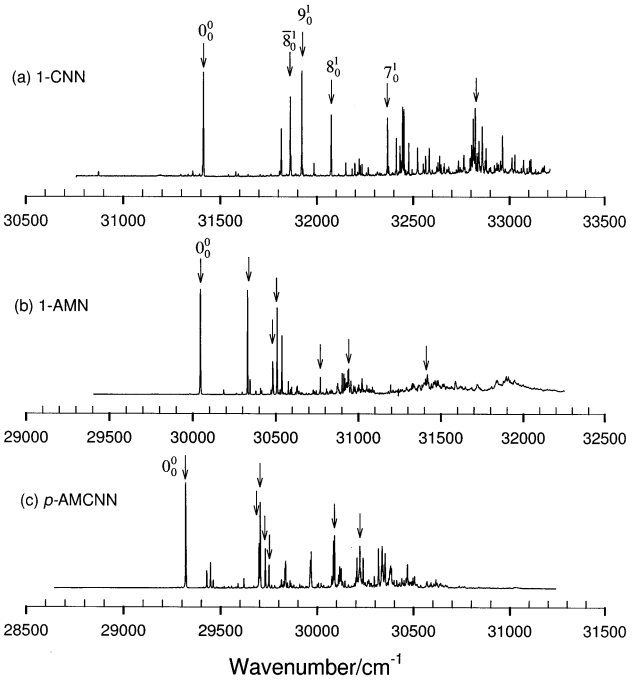

Figure 7. Fluorescence excitation spectra of substituted naphthalenes. (a) 1-cyanonaphthalene; (b) 1-aminonaphthalene; (c) 1-cyano-4-aminonaphthalene. The arrows mark the vibronic transitions whose single vibronic level fluorescence spectra are presented in this paper.

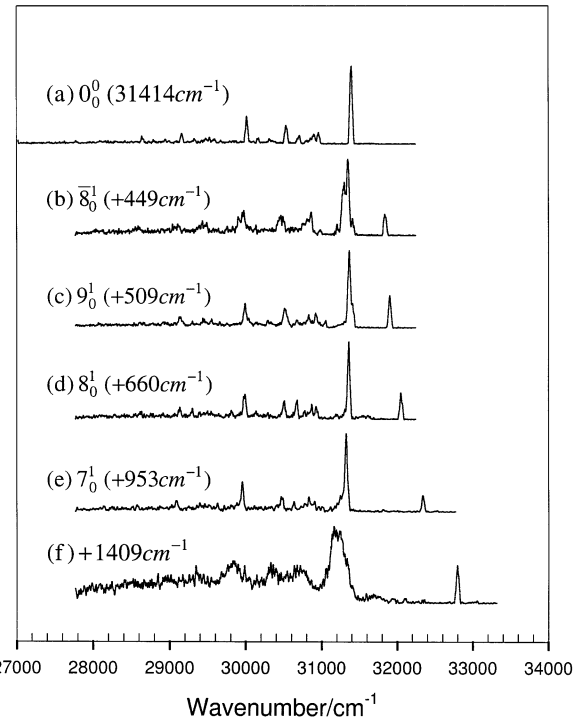

Figure 8. Dispersed fluorescence spectra of vibronic levels in 1-cyanonaphthalene. The scattered light levels at the excitation wavenumbers are: (a) negligible; (b) ∼30%; (c) ∼10%; (d) ∼20%; (e) ∼100%; (f) ∼100%.

transitions, indicating again the similarity between the potential energy surfaces of the excited and the ground states. Figure 8b,c, involving excitation of the +449, +509 cm^{-1} vibronic bands shows that the $\Delta\nu = 0$ band consists of several peaks at about −435, −495, and −533 cm^{-1} from the excitation wavelength. These are easily identified as the frequencies of these vibronic modes in the ground states. This indicates that Fermi resonance and/or Duschinski effect is occurring among

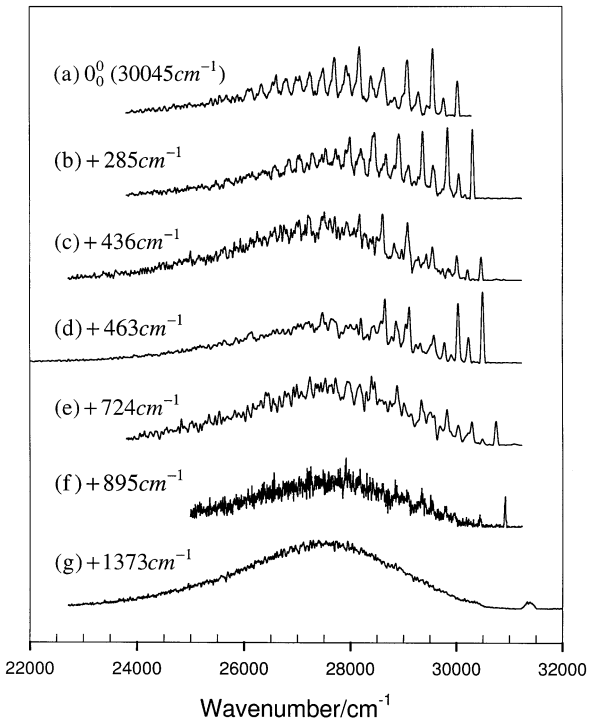

Figure 9. Dispersed fluorescence spectra of vibronic levels in 1-aminonaphthalene. The scattered light levels at the excitation wavenumbers are: (a) ∼20%; (b) ∼5%; (c) ∼5%; (d) ∼5%; (e−g) ∼100%.

these vibronic modes. The dispersed fluorescence spectra from higher excitation energies are first reported here. They are similar to the 0−0 emission with broadened bands as the excitation energy increases. Such broadening in the spectra is a result of IVR.

3.2.2. 1-AMN and p-AMCNN. The molecule 1-AMN has been studied in solution with solvents of different polarity.[31] The energy gap between the S_1 and S_2 states is about 1400 cm^{-1}.[31a] The S_1 state is an L_b type and the S_2 state is an L_a type as determined from polarization studies.[32] No similar studies on *p*-AMCNN appear in the literature, but the electronic structure of this molecule is probably similar to that of 1-AMN. The supersonic jet studies of these molecules are reported here for the first time. The fluorescence excitation spectra of these molecules (7b,c) are similar to that of 1-CNN. The congested structure in these spectra above +1000 cm^{-1} is possibly due to both mode mixing and the interaction between the S_1 and S_2 states.

The dispersed fluorescence spectra of 1-AMN and *p*-AMCNN are shown in Figures 9 and 10. They are strikingly different from those of 1-CNN, but are very similar to the emission spectra observed in aniline, 4-ABN, and benzonitrile, namely, the appearance of a broad red-shifted background that increases with excitation energy. However, in these substituted naphthalene cases, the broad background is observable at much lower excess energy. It even appears in the 0−0 emissions in these two molecules. The origin emissions consist of sharp resonant features corresponding to progressions of some vibronic modes and a broad background. The broad background gains intensity with increasing excitation energy in the +200 to +500 cm^{-1} region. The ratio between the background and the sharp features does not change monotonically in this energy region, which can be seen by comparing Figure 9b,c,d and 10b,c,d. This is similar to what was observed in aniline and 4-ABN. At 700−900 cm^{-1} of excess energy, the broad background becomes the most prominent feature and the sharp features fade away.

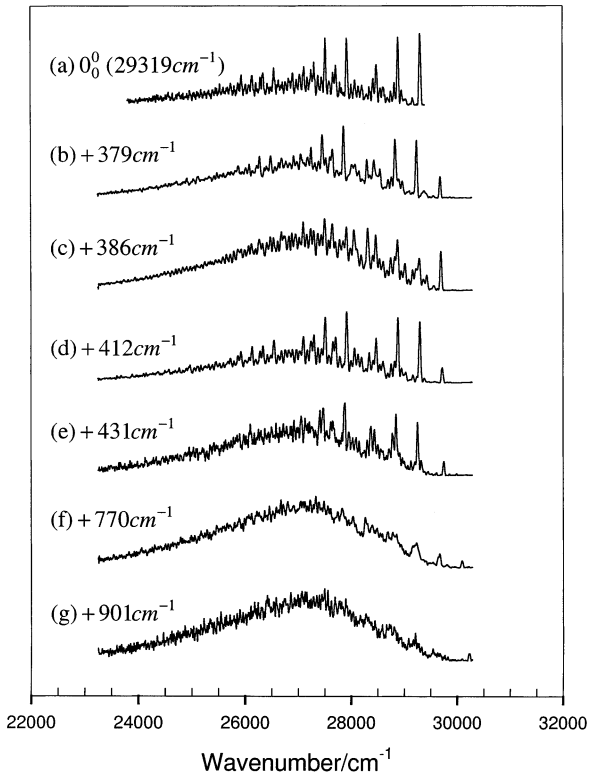

Figure 10. Dispersed fluorescence spectra of vibronic levels in 1-cyano-4-aminonaphthalene. The scattered light levels at the excitation wavenumbers are: (a) ~5%; (b) ~10%; (c) ~10%; (d) ~20%; (e−g) ~100%.

3.3. Summary of Experimental Observations. The fluorescence excitation spectra of all molecules studied in this paper have some common features. They all exhibit intense 0−0 origin transitions, with well-resolved fundamentals, overtones, and combination bands of some vibronic modes. The biggest differences lie in their dispersed fluorescence spectra. According to the dispersed fluorescence pattern at high excitation energy, they can be classified into three classes. For 4-FBN, the dispersed fluorescence spectra at all excitation energies are well structured with sharp features. For *p*-DCB and 1-CNN, the dispersed fluorescence spectra from high vibronic levels are like a broadened version of 0−0 emission, with resolvable band features; For aniline, 4-ABN, 1-AMN, and *p*-AMCNN, the dispersed fluorescence spectra from excited vibronic levels display a combination of sharp, well-resolved features and a broad background. The background grows in intensity and finally becomes the only observable feature in the spectra. However, its increase is not monotonic. The dominance of the broad background occurs at different excess energies: +1800−2000 cm^{-1} in aniline, +1500−1800 cm^{-1} in 4-ABN, and +700−900 cm^{-1} in 1-AMN and *p*-AMCNN.

4. Discussion

One of the objectives of this study was to determine the cause of the broad, unstructured red-shifted background. Is it due to IVR, spectral congestion, or emission from another excited electronic state? In IVR, all the interacting levels belong to the same electronic state while in state crossing the interacting levels belong to different electronic states. To distinguish these processes in a non time-resolved fluorescence study is not trivial, and the results of this work do not provide a definitive answer. However, our systematic study does provide some insight into to this issue.

Spectral Broadening and Congestion Due to IVR. At high excess energy, many vibronic levels may lie close in energy and the single vibronic level excitation is no longer possible. Many vibronic levels that lie within the excitation laser bandwidth can be excited either coherently or incoherently. In both cases, many levels are populated prior to emission if IVR is fast compared to emission. Each populated level will emit to its Franck−Condon allowed vibronic levels of the ground state. The resultant emission spectrum is an overlap of all the single level emission spectra of the excited vibronic levels. If the potential energy surfaces of the ground and excited states are similar and $\Delta\nu = 0$ is the most probable transition, the emissions from these vibronic levels will resemble the 0−0 emission. Due to somewhat different frequencies of vibrational modes in the ground and excited states, the 0−0 like emissions from these vibronic levels will shift in energy with respect to each other. The final emission spectrum will be an overlap of many similar patterns, but each slightly shifted. Therefore, the original sharp peaks in the single level emission will be broadened, and the emission spectrum will be a broadened version of the 0−0 emission. The dispersed fluorescence spectra of *p*-DCB and 1-CNN shown in Figure 4f,g and 8f fit this description very well.

If the potential energy surfaces between the ground and excited states shifted along some normal coordinate, there will be $\Delta\nu \neq 0$ progressions for some vibronic modes. Emission from a single level involving such vibronic modes can become quite complex compared to the 0−0 emission. Each of the progression members acts as a pseudo-origin of the 0−0 emission. The overlap of such single level emission will be more congested. As the density of vibronic states becomes high and more vibronic levels lie close in energy, extensive IVR occurs. This situation has been investigated by Zewail in *trans*-stilbene [33] and Parmenter in *p*-difluorobenzene [34]. They observed that only a broad, unstructured band existed in the emission from highly excited vibronic levels. The broad band is similar to that observed in aniline, 4-ABN, 1-AMN, and *p*-AMCNN.

The appearance of a single broad emission feature can arise from either extensive IVR or from coupling with a second electronic state with different geometry, and distinguishing between these two possibilities from a single observation is difficult. However, there are other observations that make one choice perhaps more plausible although not definitive. As discussed by the authors of previous IVR studies,[33−35] such a broad background is an indication that the IVR has reached the statistical limit. However, the nonmonotonic background intensity with excess excitation energy as observed in this study implies that the mechanism causing broadening has not reached the statistical limit and that the coupling responsible for the complete lack of structure is selective and not just energy-dependent. Figure 11 shows the density of vibronic states vs excess energy of 4-ABN calculated by a direct counting method.[36] The frequencies of the 39 vibrational modes of 4-ABN in S_1 are calculated with CASSCF(8,8)/6-31+(G,d). The dominance of the broad background starts at +1500−1800 cm^{-1} in 4-ABN (Figure 6). At this excess energy, the density of states is only from 10 to 40/cm^{-1}. The calculated frequencies for the two lowest vibrational modes are higher than the experimental values, 135 vs 92 cm^{-1} and 155 vs 124 cm^{-1}. If we replace the two lowest frequencies with the experimental values, (since the low-frequency modes contribute most to the density of states), the corrected density for +1500−1800 cm^{-1} region is 20 to 60/cm^{-1}. The S_1 state in 4-ABN belongs to the C_s symmetry group. If the symmetry of the molecule is taken into consider-

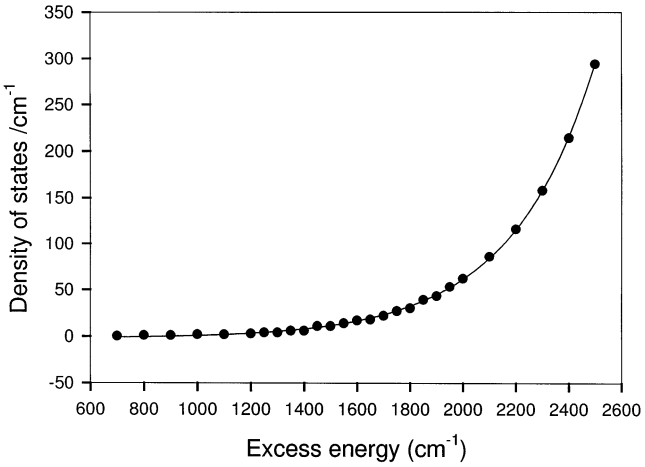

Figure 11. Vibronic density of states vs excess energy in 4-ABN, calculated by direct counting method of ref 35. The fundamental frequencies of the 39 vibrational modes in the S_1 state are calculated using CASSCF(8,8)/6-31+(G,d).

ation, the effective density will be approximately half of the calculated value. The density of states calculated for 4-ABN possibly represents an upper limit for the other substituted benzenes. This number is much smaller than the estimated 200/cm^{-1} at the onset of extensive IVR in the *trans*-stilbene study.[33]

The coupling matrix element in IVR is usually on the order of 0.1 cm^{-1},[34,37] and therefore only a few vibronic levels are coupled by IVR at such excess energy. This corresponds to a sparse or intermediate IVR case at best. It is unlikely that the emission from a few vibronic levels will give rise to such broad unstructured background, and coupling to a second electronic state seems more plausible. Indeed, the contributions from hundreds or even thousands of zero-order vibronic levels are required to produce such congested background emission based upon previous spectral simulations in IVR studies of similar molecules.[29,34c] The estimation of the density of states neglect rotational and vibrational coupling. Such coupling can be important for high *J* levels. In a supersonic jet, the molecules occupy a small set of low *J* levels due to the rotational cooling and the ro-vibrational coupling is expected to be small.

The broadening of individual features in Figure 6d,g of 4-ABN does indicate that IVR occurs in these molecules and contributes to the congestion of the background. However, IVR is probably not the only source of the unstructured background in aniline and 4-ABN. The broad background in the dispersed fluorescence spectra of 1-AMN and *p*-AMCNN is unlikely to be caused by IVR since the background is even observable from 0−0 emission (Figures 9a and 10a). The nonmonotonic behavior of the broad background with excess energy implies that it is not simply due to spectral congestion. Finally, the rise in the broad, red-shifted background is accompanied by disappearance of the structured features closer in frequency to the excitation frequency. This cannot be due to spectral congestion and is hard to explain by pure IVR.

While IVR certainly occurs in these molecules, in summary there are three observations that suggest that coupling with a second electronic state is also important in some cases: the fact that the broadening is nonmonotonic in excitation energy and therefore depends on some selective coupling, the relatively low density of vibrational states at the excitation energies where loss of structure is observed, and the loss of structured features near the excitation frequency where the emission spectrum is relatively clean.

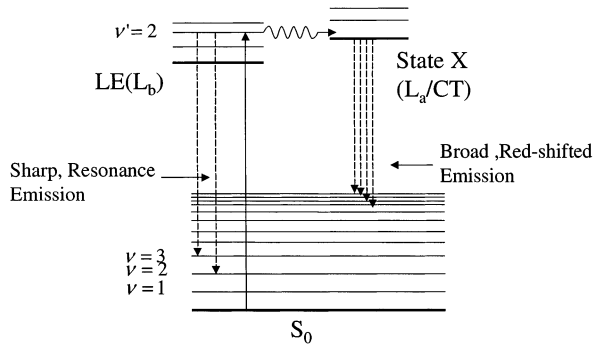

Figure 12. Illustration of the proposed three-state model. The potential surface of the S_1(LE) and the ground state are similar, and the emission from the S_1 state shows primarily sharp features. State X (L_a/CT) has a shifted potential surfaces along some molecular coordinate due to its charge-transfer character, and the emission will be broad and red-shifted with respect to that from the LE state.

Emission from Another Electronic State. If IVR and spectral congestion are insufficient to explain our observations, coupling to a third electronic state with a different geometry from the LE state is necessary. We propose a three-state model to explain the broad background observed in aniline, 4-ABN, 1-AMN, and *p*-AMCNN similar to the one discussed by Mordzinski et al.[15] The idea is illustrated in Figure 12. The three states are the ground electronic state, a locally excited electronic state (LE) with potential surface similar to that of the ground state, and a second excited electronic state (state X) with an equilibrium geometry significantly different from the other two states. The emission spectrum from the locally excited state will be dominated by $\Delta v = 0$ and $\Delta v =$ small Franck−Condon factors, producing sharp features that are relatively unshifted from the excitation frequency. State X cannot be directly excited at these wavenumbers due to poor Franck−Condon factors between the zero-point level of the ground state and low-lying vibrational levels of state X. It can be populated by internal conversion from populated levels of the locally excited state, as long as state X is lower in energy at some geometry. The emission from this state X to the repulsive potential energy surface of the ground state will be red-shifted, and dominated by $\Delta v =$ large Franck−Condon factors, producing the broad red-shifted background. Thus, exciting high vibronic levels in a locally excited state will give rise to dual fluorescence. The state crossing as depicted in Figure 12 may be too dramatic. In fact, dual fluorescence is possible as long as there is significant mixing between the two excited electronic states. The extensive mixing between the two states may occur if they are close in energy at some geometry. How close they must be in energy to achieve the required mixing depends on the strength of the coupling, which is unknown.

Our study of substituted benzenes and naphthalenes offers some information regarding the nature of the state X, but such information is far from definitive. Such a state exists in the molecules containing electron-donating and/or electron-withdrawing substituents, such as aniline, 4-ABN, 1-AMN, *p*-AMCNN presented here, and benzonitrile, and tolunitrile studied by Mordzinski et al.[15] There is a charge-transfer (CT) state in these molecules consisting of $\pi_{ring} \rightarrow A^*$ and $D \rightarrow \pi_{ring}^*$ type configuration (refer to introduction part for the notations). The transition dipole moment from the ground state to this CT state, if allowed, will be parallel to the axis of substitution that is also parallel to the transition dipole moment of the ^1L_a state (the second $\pi_{ring} \rightarrow \pi_{ring}^*$ excited state in Platt's nomenclature) and perpendicular to that of the ^1L_b state. This means that the

CT and ^1L_a states belong to the same symmetry representation and the ^1L_b belongs to a different one.

The molecular eigenstates S_i ($i = 1.2.3...$) will be a combination of all these zero-order states. The S_1 state will be primarily ^1L_b because of the small interaction with other zero-order states due to different symmetry, justifying the name of locally excited state. The S_2 state on the other hand will be ^1L_a with some CT character because of possible configuration interaction between them. The extent of CT character will depend on coupling and energy gap between the L_a and CT states. The energy of S_2 in these substituted molecules is also stabilized by such an interaction, and the energy gap between S_1 and S_2 is expected to be less than that of the parent aromatic molecules. (9000 cm^{-1} for benzene and 3900 cm^{-1} for naphthalene). Such an S_2 made up of a mixture of ^1L_a and CT states will have a different geometry than that of the ground state, and it is a possible candidate for the state X.

This assumption, if correct, will explain other experimental observations such as the appearance of a broad background at lower excess energy in 1-AMN and *p*-AMCNN than in substituted benzenes. In naphthalene, the energy gap between ^1L_b and ^1L_a is much smaller than in benzene. Therefore, in substituted benzenes and naphthalenes, the energy gap between S_1 and S_2 is expected to be smaller in the substituted naphthalenes.

For 4-FBN and *p*-DCB with para-positioned electron withdrawing groups on the same aromatic ring, the zero-order charge-transfer configuration is expected to be high in energy due to the competition of the electron withdrawing groups. The S_2 (^1L_a) in these molecules will have less CT character than in aniline and 4-ABN. The energy gap between S_1 and S_2 will be larger, and the dominance of the broad background will occur at higher excitation energies. The more congested background in emission spectra from vibronic levels involving mode 3 may be partially due to vibronic coupling to the S_2 state. Mode 3, which belongs to b_{3g}, gains transition probability through vibronic coupling to an L_a type excited state.

In 1-CNN (as opposed to benzonitrile), emission from highly excited vibronic levels close to the onset of S_2 displays only IVR with no strong broad background indicating S_2 in 1-CNN is also a locally excited state with geometry similar to that of S_1 and the ground state. This may be due to a smaller admixture of the CT state. The CT configuration in 1-CNN and benzonitrile is $\pi_{ring} \rightarrow \pi_{-CN}^*$. In both benzonitrile and 1-CNN, π_{-CN}^* has approximately the same energy, but π_{ring} and π_{ring}^* have lower energy in the naphthalenes. This means that in 1-CNN, the CT zero-order state will be higher in energy than its counterpart in benzonitrile, while the L_b and L_a zero-order states are at lower energies. Thus, the energy gap between the CT state and the L_a and L_b states will be larger in 1-CNN, and the interaction among them will be smaller. As a result, the S_2 state in 1-CNN will have less CT character..

Another issue needs to be addressed. The growth of the broad background with increasing excitation energy is not monotonic. It would be interesting to know whether level mixing between two electronic states is mode-selective or whether it depends on an accidental near-coincidence in energy between two vibronic states. Unfortunately, there is no solid evidence in our study that helps to answer this question. Level mixing is seemingly enhanced by a combination mode of 13 and 6a in aniline (Figure 5e), but that is not the case in 4-ABN. It is more likely that this nonmonotonic growth of the background indicates that the level mixing has not reached the statistical limit. At the onset of level mixing, the density of states of the accepting levels (vibronic levels of the L_a/CT state in this case) is not high, and the coupling between the localized and accepting levels may depend on accidental degeneracy.

5. Conclusion

Dual fluorescence has been observed in aniline, 4-aminobenzonitrile, 1-aminonaphthalene, and 1-amino-4-cyanonaphthalene in a supersonic jet. The broad, unstructured, and red-shifted background is difficult to explain by only IVR or spectral congestion. We propose that it is due to emission from an L_a state with some admixture of a CT state. The mixed state would have a potential surface shifted with respect to that of the ground state. The L_a state is populated through internal conversion from a locally excited state. The onset of this process starts at different excess energy in different molecules: $+1800-2000$ cm^{-1} in aniline, $+1500-1800$ cm^{-1} in 4-aminobenzonitrile, and $+700-900$ cm^{-1} in 1-aminonaphthalene and 1-amino-4-cyanonaphthalene.

References and Notes

(1) (a) Coulson, A. *Valence*; Oxford University Press: London, 1952. (b) Nagakura, S.; Tanaka, J. *J. Chem. Phys*. **1954**, *22*, 236.

(2) (a) Chattoraj, M.; Bal, B.; Closs, G. L.; Levy, D. H. *J. Phys. Chem*. **1991**, *95*, 9666. (b) Chattoraj, M.; Bal, B.; Shi, Y.; Closs, G. L.; Levy, D. H. *J. Phys. Chem*. **1993**, *97*, 13046.

(3) (a) Syage, J. A.; Felker, P. M.; Zewail, A. H. *J. Chem. Phys*. **1984**, *81*, 2233. (b) van Dantzig, N. A.; Shou, H.; Alfano, J. C.; Yang, N. C.; Levy, D. H. *J. Chem. Phys*. **1994**, *100*, 7068.

(4) Russell, T. D.; Levy, D. H. *J. Phys. Chem*. **1982**, *86*, 2718.

(5) Kobayashi, T.; Futakami, M.; Kajimoto, O. *Chem. Phys. Lett.* **1987**, *141*, 450.

(6) Carsey, T. P.; Findley, G. L.; McGlynn, S. P. *J. Am. Chem. Soc*, **1979**, *101*, 4502.

(7) Here is a list of the most recent experimental studies on 4-DMABN. (a) Lommatzsch, U.; Gerlach, A.; Lahmann, C.; Brutschy, B. *J. Phys. Chem. A* **1998**, 6421. (b) Perez Salgado, F.; Herbrich, J.; Kunst, G. M.; Rettschnick, R. P. H. *J. Phys. Chem. A* **1999**, 3184. (c) Chudoba, C.; Kummmrow, A.; Dreyer, J.; Stenger, J.; Nibbering, E. T. J.; Elsaesser, T.; Zachariasse, K. A. *Chem. Phys. Lett*. **1999**, 357. (d) Dreyer, J.; Kummrow, A. *J. Am. Chem. Soc*. **2000**, *122*, 2577. (e) Kwok, W. M.; Ma, C.; Phillips, D.; Matousek, P.; Parker, A. W.; Towrie, M. *J. Phys. Chem. A* **2000**, *104*, 4188.

(8) (a) Lippert, E.; Lüder, W.; Moll, F.; Nägele, W.; Boos, H.; Prigge, H.; Seibold-Blankenstein, I. *Angew. Chem*. **1961**, *73*, 695. (b) Lippert, E.; Lüder, W.; Boos, H. In *Advances in Molecular Spectroscopy*; Mangini, A., Ed.; Pergamon Press: Oxford, 1962; p 443.

(9) (a) Rotkiewicz, K.; Grellmann, K. H.; Grabowski, Z. R. *Chem. Phys. Lett*. **1973**, *19*, 315. (b) Rotkiewicz, K.; Grellmann, K. H.; Grabowski, Z. R. *Chem. Phys. Lett*. **1973**, *21*, 212. (c) Siemiaczuk, A.; Grabowski, Z. R.; Krowczyñski, A.; Asher, M.; Ottolengui, M. *Chem. Phys. Lett*. **1977**, *51*, 315.

(10) (a) Kobayashi, T.; Futakami, M.; Kajimoto, O. *Chem. Phys. Lett*., **1986**, *130*, 63. (b) Kajimoto, O.; Nayuki, T.; Koboyashi, T. *Chem. Phys. Lett*. **1993**, *209*, 357.

(11) (a) Gibson, E. M.; Jones, A. C.; Phillips, D. *Chem. Phys. Lett*. **1988**, *146*, 270. (b) Gibson, E. M.; Jones, A. C.; Taylor, A. G.; Bouwman, W. G.; Phillips, D.; Sandell, J. *J. Phys. Chem*. **1988**, *92*, 5449. (c) Howell, R.; Taylor, A. G.; Joslin, E. M.; Phillips, D. *J. Chem. Soc., Faraday*. Trans. **1992**, *88*, 1605. (d) Yu, H. P.; Joslin, E.; Crystal, B.; Smith, T.; Sinclair, W.; Phillips, D. *J. Phys. Chem.* **1993**, *97*, 8146.

(12) Peng, L. W.; Dantus, M.; Zewail, A. H.; Kemnitz, K.; Hicks, J. M.; Eisenthal, K. *J. Phys. Chem.* **1987**, *91*, 6162.

(13) (a) Warren, J. A.; Bernstein, E. R.; Seeman, J. I. *J. Chem. Phys*. **1988**, *88*, 871. (b) Grassian, V. H.; Warren, J. A.; Bernstein, E. R. *J. Chem. Phys.* **1989**, *90*, 3994.

(14) (a) Leinhos, U.; Künler, W.; Zachariasse, K. A. *J. Phys. Chem*. **1991**, *95*, 2013. (b) Zachariasse, K. A.; Grobys, M.; Von der Haar, Th.; Hebecker, A.; V.Il'ichev, Yu.; Jiang, Y.-B.; Morawski, O.; Kühnle, W. J. *Photochem. Photobiol. A: Chem.* **1996**, *102*, 59. (c) V.Ill'ichev, Yu.; Kühnle, W. J.; Zachariasse, K. A. *J. Phys. Chem. A* **1998**, *102*, 5670.

(15) Mordzinski, A.; Sobolewski, A. L.; Levy, D. H. *J. Phys. Chem.* **1997**, *101*, 8221.

(16) Sakota, K.; Nishi, K.; Ohashi, K.; Sekiya, H. *Chem. Phys. Lett*. **2000**, *322*, 407.

(17) Sobolewski, A. L.; Domcke, W. *Chem. Phys. Lett*. **1996**, *250*, 428.

(18) Sobolewski, A. L.; Sudholt, W.; Domcke, W. *J. Phys. Chem. A* **1998**, *102*, 2716.

(19) (a) Smalley, R. E.; Levy, D. H.; Wharton, L. *J. Chem. Phys.* **1976**, *64*, 3266. (b) Sharfin, W. K.; Johnson, E.; Levy, D. H. *J. Chem. Phys.* **1979**, *71*, 1292.

(20) Fujita, K.; Fujiwara, T.; Matsunage, K.; Ono, F.; Nakajima, A.; Watanabe, H.; Koguchi, T.; Suzuka, I.; Matsuzawa, H.; Iwata, S.; Kaya, K. *J. Phys. Chem*. **1992**, *96*, 10693.

(21) (a) Powers, D. E.; Hopkins, J. B.; Smalley, R. E. *J. Chem. Phys*. **1980**, *72*, 5721. (b) Mikami, N.; Hiraya, A.; Fujiwara, I.; Ito, M. *Chem. Phys. Lett*. **1980**, *74*, 531.

(22) Chernoff, D. A.; Rice, S. A. *J. Chem. Phys.* **1979**, *70*, 2511.

(23) The assignment of vibronic structure in 4-FBN is based on the following works: (a) Tan, H. T.; Thistlethwaite, P. J. *J. Chem. Phys*. **1973**, *58*, 4408. (b) Green, J. H. S.; Harrison, D. J. *Spectrochim. Acta* **1976**, *32A*, 1279. (c) Pavan Kumar, A.; Ramana Rao, G. *Spectrochim. Acta, Part A* **1997**, *53*, 2023. The assignment of *p*-DCB is based on (a) Barraclough, C. G.; Bissett, H.; Pitman, P.; Thistlethwaite, P. J. *Aust. J. Chem*. **1977**, *30*, 753. (b) Castro-Pedrozo, M. C.; King, G. W. *J. Mol. Spectrosc*. **1978**, *73*, 386. (c) Pavan Kumar, A.; Ramana Rao, G. *Spectrochim. Acta, Part A* **1997**, *53*, 2033. The assignment of aniline is based on ref 21. The assignment of 4-ABN is based on ref 11d.

(24) Fitch, P. H.; Haynam, C. A.; Levy, D. H. *J. Chem. Phys*. **1981**, *74*, 6612.

(25) Hopkins, J. B.; Powers, D. E.; Smalley, R. E. *J. Chem. Phys*. **1980**, *72*, 2905; Hopkins, J. B.; Powers, D. E.; Smalley, R. E. *J. Chem. Phys*. **1980**, 72, 5039; Hopkins, J. B.; Powers, D. E.; Smalley, R. E. *J. Chem. Phys*. **1980**, *72*, 5049; Hopkins, J. B.; Powers, D. E.; Smalley, R. E. *J. Chem. Phys*. **1980**, *73*, 683.

(26) Saigusa, H.; Itoh, M. *J. Chem. Phys.* **1984**, *81*, 5692.

(27) Lahmani, F.; Zehnacker-Rentien, A.; Breheret, E. *J. Chem. Soc., Faraday Trans.* **1993**, *89*, 623.

(28) Warren, J. A.; Hayes, J. M.; Small, G. J. *J. Chem. Phys*. **1983**, *80*, 1786.

(29) Beck, S. M.; Powers, D. E.; Hopkins, J. B.; Smalley, R. E. *J. Chem. Phys.* **1980**, *73*, 2019.; Beck, S. M.; Powers, D. E.; Hopkins, J. B.; Smalley, R. E. *J. Chem. Phys.* **1981,** *74*, 43.

(30) (a) Suzuki, S.; Fuiji, T.; Ishikawa, T. *J. Mol. Spectrosc*. **1975**, *57*, 490. (b) Whipple, M. R.; Vasak, M.; Michl, J. *J. Am. Chem. Soc*. **1978,** *100*, 6844.

(31) (a) Meech, S. R.; O'Connor, D. V.; Phillips, D.; Lee, A. G. *J. Chem. Soc., Faraday Trans II* **1983**, *79*, 1563. (b) Dresner, J.; Modiano, S. H.; Lim, E. C. *J. Phys. Chem*. **1992**, *96*, 4310. (c) Suzuki, K.; Tanabe, H.; Tobita, S.; Shizuka, H. *J. Phys. Chem. A* **1997**, *101*, 4496.

(32) Chakrabarti, S. K. *J. Mol. Struct*. **1971**, *7*, 455.

(33) Felker, P. M.; Lambert, W. R.; Zewail, A. H. *J. Chem. Phys*. **1985**, *82*, 3003.

(34) (a) Coveleskie, R. A.; Dolson, D. A.; Parmenter, C. S. *J. Phys. Chem*. **1985**, *89*, 645; Coveleskie, R. A.; Dolson, D. A.; Parmenter, C. S. *J. Phys. Chem.* **1985**, *89*, 655. (b) Holtzcaw, K. W.; Parmenter, C. S. *J. Chem. Phys*. **1986**, 84, 1099. (c) Dolson, D. A.; Holtzclaw, K. W.; Moss, D. B.; Parmenter, C. S. *J. Chem. Phys*. **1986**, *84*, 1119.

(35) Felker, P. M.; Zewail, A. H. *Adv. Chem. Phys*. **1988**, *70*, 265.

(36) Stein, E. S.; Rabinovitch, B. S. *J. Chem. Phys.* **1973**, *58*, 2438

(37) Smalley, R. E. *Annu. Rev. Phys. Chem.* **1984**, *34*, 129.